Research Article

Cancer Immunology Research

Cellular Cytotoxicity of Next-Generation CD20 Monoclonal Antibodies

Karl R. VanDerMeid[1], Michael R. Elliott[2], Andrea M. Baran[3], Paul M. Barr[1], Charles C. Chu[1], and Clive S. Zent[1]

Abstract

CD20 monoclonal antibodies (CD20 mAb) induce cellular cytotoxicity, which is traditionally measured by antibody-dependent cellular cytotoxicity (ADCC) assays. However, data suggest that antibody-dependent cellular phagocytosis (ADCP) is the primary cytotoxic mechanism. We directly compared *in vitro* ADCP versus ADCC using primary human cells. After establishing the primacy of ADCP, we examined next-generation CD20 mAbs, including clinically relevant drug combinations for their effects on ADCP. ADCP and ADCC induction by rituximab, ofatumumab, obinutuzumab, or ocaratuzumab was measured using treatment-naïve chronic lymphocytic leukemia (CLL) target cells and either human monocyte-derived macrophages (for ADCP) or natural killer (NK) cells (for ADCC). Specific effects on ADCP were evaluated for clinically relevant drug combinations using BTK inhibitors (ibrutinib and acalabrutinib), PI3Kδ inhibitors (idelalisib, ACP-319, and umbralisib), and the BCL2 inhibitor venetoclax. ADCP (∼0.5–3 targets/macrophage) was >10-fold more cytotoxic than ADCC (∼0.04–0.1 targets/NK cell). ADCC did not correlate with ADCP. Next-generation mAbs ocaratuzumab and ofatumumab induced ADCP at 10-fold lower concentrations than rituximab. Ofatumumab, selected for enhanced complement activation, significantly increased ADCP in the presence of complement. CD20 mAb-induced ADCP was not inhibited by venetoclax and was less inhibited by acalabrutinib versus ibrutinib and umbralisib versus idelalisib. Overall, ADCP was a better measure of clinically relevant mAb-induced cellular cytotoxicity, and next-generation mAbs could activate ADCP at significantly lower concentrations, suggesting the need to test a wide range of dose sizes and intervals to establish optimal therapeutic regimens. Complement activation by mAbs can contribute to ADCP, and venetoclax, acalabrutinib, and umbralisib are preferred candidates for multidrug therapeutic regimens. *Cancer Immunol Res; 6(10); 1150–60. ©2018 AACR.*

Introduction

Unconjugated CD20 monoclonal antibodies (CD20 mAb) have an important role in the treatment of B-cell malignancies and autoimmune diseases (1, 2). However, the mechanisms of CD20 mAb-induced B-cell cytotoxicity are not fully understood. Type I CD20 mAbs (e.g., rituximab, ofatumumab, and ocaratuzumab) have minimal direct cytotoxicity for primary malignant B cells (3–5). The direct cytotoxic effects of the type II CD20 mAbs are controversial, with conflicting reports of direct cytotoxicity (6) and absence of significant cytotoxicity in primary B cells (7, 8). In contrast, CD20 mAbs can be effective at activating innate immune cytotoxic mechanisms, including complement-dependent cytotoxicity (CDC), antibody-dependent cellular phagocytosis (ADCP), and antibody-dependent cellular cytotoxicity (ADCC). A detailed understanding and comparison of these cellular cytotoxic mechanisms induced by CD20 mAbs is essential for designing combination therapies to achieve optimal patient outcomes.

The relative contribution of CD20 mAb-mediated ADCC and ADCP to therapeutic efficacy is not well defined. Cellular cytotoxicity of the prototypic CD20 mAb, rituximab, was initially evaluated by ADCC assays using unsorted human peripheral blood mononuclear effectors cells and target cells from CD20-expressing lymphoma lines. Rituximab induced lysis of ∼50% of target cells (9). Subsequent studies showed that natural killer (NK) cells are the primary peripheral blood effector cells performing ADCC, whereas monocytes and neutrophils have minimal cytotoxic activity (10, 11). In contrast, *in vivo* murine studies of CD20 mAb-mediated clearance of circulating B cells show a major role for ADCP by fixed hepatic macrophages (Kupffer cells), with minimal NK cell–mediated cytotoxicity (12–17). These data suggest that clearance of opsonized B cells could be similar to that of autoantibody opsonized blood cells, which are efficiently cleared by ADCP in the liver and spleen in human autoimmune hemolytic anemia and immune thrombocytopenia (18, 19). The primary role of ADCP in the clearance of opsonized target cells from the circulation is further supported by published data showing that human monocyte-derived macrophages (hMDM) are capable of executing rapid phagocytosis of multiple mAb-ligated chronic lymphocytic leukemia (CLL) cells (8). Next-generation CD20 mAb development has focused on optimizing ADCC (20–22). Defining the relative contribution of ADCC and ADCP as mediators of CD20-mediated cytotoxicity is needed so that the most relevant preclinical drug data can be generated and used for clinical trial design.

[1]Division of Hematology/Oncology, Wilmot Cancer Institute, University of Rochester Medical Center, Rochester, New York. [2]Department of Microbiology and Immunology, Center for Vaccine Biology and Immunology, University of Rochester Medical Center, Rochester, New York. [3]Department of Biostatistics and Computational Biology, University of Rochester Medical Center, Rochester, New York.

Corresponding Author: Clive S. Zent, University of Rochester Medical Center, 601 Elmwood Avenue, Box 704, Rochester, NY 14642. Phone: 585-273-3258; Fax: 585-273-1042; E-mail: Clive_Zent@urmc.rochester.edu

doi: 10.1158/2326-6066.CIR-18-0319

©2018 American Association for Cancer Research.

Downloaded from http://aacrjournals.org/cancerimmunolres/article-pdf/6/10/1150/2343068/1150.pdf by guest on 23 April 2024

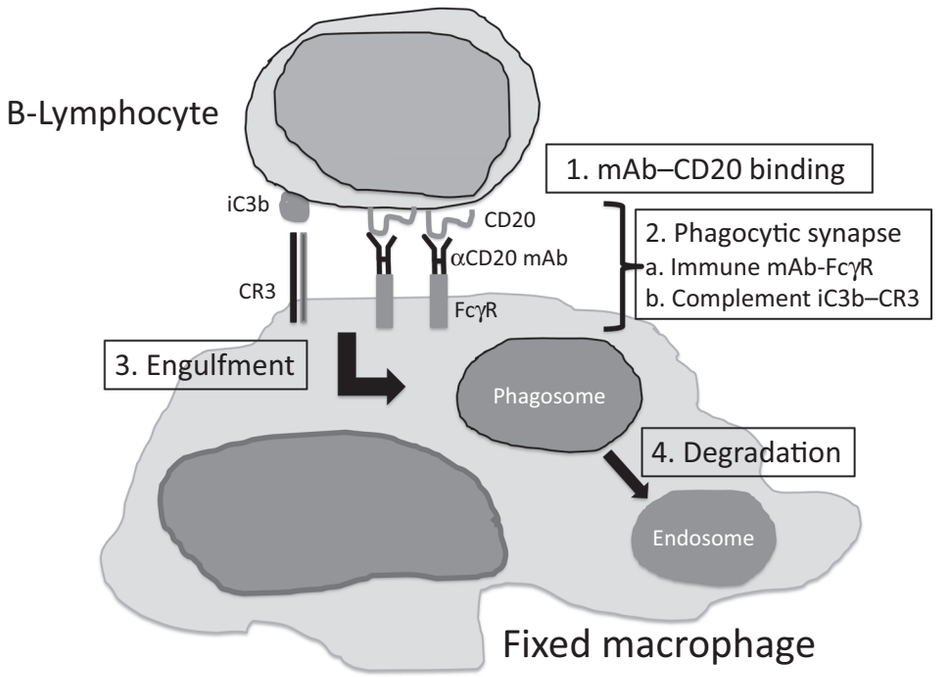

Figure 1.
ADCP. Illustration: ADCP of B lymphocytes by human monocyte-derived macrophages (hMDMs, fixed macrophage) occurs via sequential steps. CD20 monoclonal antibody (CD20 mAb) opsonizing the B-lymphocyte membrane can bind the hMDM Fc gamma receptor (FcγR) to form an immune synapse. Complement activating mAbs can generate complement C3 activation fragments (iC3b) that ligate hMDM membrane complement receptor 3 (CR3) to form a complement synapse. Synapse formation can result in B-lymphocyte engulfment to form an intracellular phagosome.

Limited data exist on the parameters that mediate phagocytosis of mAb-ligated B cells by human macrophages. ADCP initiated by a CD20 mAb requires multiple sequential steps (detailed in Fig. 1). The prototype chimeric CD20 mAb rituximab has a murine Fab and human wild-type IgG1κ constant regions (23). Next-generation CD20 mAbs were selected (e.g., ofatumumab; refs. 24, 25) or bioengineered (e.g., ocaratuzumab; refs. 21, 22) to increase binding efficacy to CD20 (Table 1). Fc regions were manipulated to increase FcR affinity by defucosylation (e.g., obinutuzumab; ref. 20) or amino acid engineering (e.g., ocaratuzumab; refs. 21, 22). We selected these mAbs for detailed investigations because rituximab, ofatumumab, and obinutuzumab are FDA approved, and ocaratuzumab has been evaluated in several clinical trials.

CD20 mAbs with wild-type Fc (rituximab and ofatumumab) activate complement and mediate CDC, whereas Fc-modified obinutuzumab and ocaratuzumab have minimal complement activating activity (20, 21). Complement activation by rituximab or ofatumumab results in covalent binding of C3 fragments (C3b, iC3b, and C3dg) to target cell membranes (5, 26). iC3b is the natural ligand of macrophage complement receptor 3 (CR3; aka integrin $\alpha_M\beta_2$, CD11b/CD18; ref. 27). The iC3b–CR3 synapse significantly increases macrophage phagocytosis of opsonized bacteria (27). In contrast, limited data are available on the role of complement activation on inducing ADCP (28).

Targeted small-molecule inhibitors, including ibrutinib, idelalisib, and venetoclax, have improved treatment options for patients with CLL but are not curative. Combinations of targeted therapy and CD20 mAb therapy have been shown to be tolerable and effective in clinical trials (29–31). However, studies suggest that the Bruton tyrosine kinase (BTK) inhibitor ibrutinib and the phosphoinositide-3-kinase delta (PI3Kδ) inhibitor idelalisib decrease ADCP (32–34). In contrast, data from semiquantitative assays show that the more specific BTK inhibitor acalabrutinib has less inhibitory activity on ADCP than ibrutinib (35). These findings suggest that off-target effects of ibrutinib, including inhibition of non-BTK members of the Tec protein tyrosine kinase (TEC) family molecules, could inhibit hMDM-mediated ADCP (36). An improved understanding of the effects of targeted small-molecule drugs on macrophage phagocytosis is required for designing combination therapy regimens, including CD20 mAb.

We assessed CD20 mAb-mediated cellular cytotoxicity of primary CLL cells by autologous or allogeneic (healthy donor) effector cells to test the following hypotheses: (i) ADCP is the primary mechanism of cellular cytotoxicity by CD20 mAb and cannot be predicted by ADCC; (ii) higher binding affinity for CD20 (e.g., ocaratuzumab) results in higher ADCP at lower mAb concentrations; (iii) mAb activation of complement can increase ADCP; and (iv) novel small-molecule–targeted BCR pathway

Table 1. Comparison of CD20 mAb construction, binding characteristics, and ability to activate complement

	Construction	CD20-binding efficiency (kD)	FcγR affinity (kD)	Complement activation
Rituximab	Chimeric (murine Fab) WT human IgG1Fc	+ (5–8) Faster off rate $t_{1/2}$ = 0.7 h	+ (660)	+
Ofatumumab	Fully human WT IgG1 Fc	++ (3–6) Slow off rate $t_{1/2}$ = 4 h	+ (NA)	++
Obinutuzumab	Humanized Fab Defucosylated IgG1 Fc	+ (4)	++ (55)	±
Ocaratuzumab	Mutant humanized Fab Mutant human IgG1Fc	++ (0.097) Slow off rate	++ (NA)	±

Abbreviations: Fab, variable region; Fc, fragment crystallizable; FcR, Kd data for FcRIII; Kd, dissociation constant in nmol/L; NA, not available; $t_{1/2}$, half-life; WT, wild-type.

Downloaded from http://aacrjournals.org/cancerimmunolres/article-pdf/6/10/1150/2343068/1150.pdf by guest on 23 April 2024

inhibitors cause less inhibition of CD20 mAb-mediated ADCP than the available BCR pathway inhibitors ibrutinib or idelalisib. Our data support validation of these hypotheses. These preclinical data can be used for the design of future clinical trials that test combination therapies and for the development of regimens that can improve patient outcome.

Materials and Methods

Patient and volunteer donor samples

This study was conducted at the Wilmot Cancer Institute of the University of Rochester with approval of the Institutional Research Subjects Review Board according to the ethical guidelines of the Declaration of Helsinki. All specimens were used with written informed consent. Patient blood samples were collected from 41 treatment-naïve patients with CLL diagnosed using standard criteria (37) and 17 healthy blood donors.

Patient-derived monocytes and CLL isolation

Autologous monocytes were isolated by positive selection from CLL patient peripheral blood as previously described with minor modification (8). In brief, peripheral blood mononuclear cells (PBMC) were isolated from 20 to 30 mL of fresh EDTA anticoagulated whole blood by density gradient centrifugation (Ficoll-Paque PLUS, GE Healthcare). Monocytes were then selected using 0.5 mL of CD14-positive selection beads (BD Biosciences) in a selection buffer composed of 2 mmol/L ethylenediaminetetraacetic acid (EDTA; J.T. Baker Inc.), 2% heat-inactivated fetal bovine serum (HI-FBS; Sigma-Aldrich) in Dulbecco's phosphate-buffered saline (DPBS; Corning cellgro). Monocytes were collected with "The Big Easy" EasySep magnet (Stemcell Technologies) into 14 mL Falcon tubes (Corning) using the EasySep (Stemcell Technologies) positive selection procedure. Purified monocytes (median, 87%; range, 77–98) were used to establish cultures within 2 hours of specimen collection.

The CD14-negative PBMC fraction underwent negative selection to a CLL cell purity of $\geq$80% using 0.2 mL of Human B-cell Enrichment beads without CD43 depletion beads (Stemcell Technologies) and the EasySep negative selection procedure in selection buffer. CLL cells were stored within 4 hours of process initiation in CryoStor CS5 (Biolife Solutions) and frozen in a Cryo-1° Freezing container (Nalgene) overnight at −80°C and then stored long term in liquid nitrogen. Stored CLL cells had a median purity of 91% (range, 74%–99%), determined by flow-cytometric measurement of the cells coexpressing CD19 (clone SJ25C1; BioLegend) and CD5 (clone UCHT2; BD Biosciences) as previously described (8). CLL cell viability (median, 90%; range, 80%–98%) after thawing and prior to use was measured by trypan blue (Amresco) staining as previously described (8).

Healthy donor-derived monocyte and NK cell isolation

Healthy donor blood cells were collected from 17 freshly discarded whole blood leukoreduction filters (Sepacell RS-2000; Fenwal Inc.) after being used to process volunteer donor whole blood (American Red Cross). Monocytes and NK cells were collected using a modification of previously described techniques (38, 39). In brief, the filter was gently flushed through the outflow tube with a total of 50 mL of selection buffer in 10 mL aliquots with a dwell time of 5 minutes each. The filtrate was then layered onto Ficoll-Paque PLUS (GE Healthcare) to concentrate the mononuclear cells. Monocytes (mean purity 95%) were then isolated by positive selection as described for the patient-derived monocytes and then either used immediately to generate macrophages or cryopreserved in Cryostor CS5. NK cells (mean purity 51%) were isolated from the remaining cells by negative selection with Human NK Cell Enrichment beads (BD Biosciences) supplemented with EasySep positive selection for CD3 (Stemcell Technologies) to remove additional T cells by the same method as used for selection of autologous CLL cells. NK cells were then immediately frozen in CryoStor CS5.

CD20 monoclonal antibodies

Rituximab and obinutuzumab (Genentech), ofatumumab (Novartis), and alemtuzumab (Sanofi Genzyme) were obtained from the University of Rochester Medical Center pharmacy. Ocaratuzumab was generously provided by Mentrik Biotech.

ADCP assay

ADCP was assayed using our previously published method (8). In brief, 3×10^5 peripheral blood monocytes were cultured per well of a 96-well plate (Costar) and matured into hMDMs in RPMI-1640 (Corning Cellgro) supplemented with L-glutamine, penicillin, and streptomycin (Gibco, Life Technologies), 10% FBS, and M-CSF (10 ng/mL; PeproTech) over 5 to 6 days, with a 50% volume medium change at day 3. The culture was then continued for an additional 2 days with M-CSF (10 ng/mL) and IL10 (10 ng/mL; PeproTech). On the day of the experiment, CLL cells were thawed, washed 2 times to remove freezing medium, and stained with PKH26 (Sigma-Aldrich) as per manufacturer instructions. The stained CLL cells were incubated for a minimum of 1 hour at 37°C with 5% CO_2 prior to testing. The effector hMDMs were then cocultured with purified CLL cell targets at an effector to target ratio of 1:5 for 3 hours in 10% C5-deficient serum (Complement Technology), to allow for deposition of C3 activation fragments but not the formation of lytic membrane attack complexes, and CD20 mAb (10 μg/mL). We previously found that these parameters optimized the assay for comparison of the ADCP achieved by different CD20 mAbs (8).

At the completion of the coculture, all the cells from each well were mechanically harvested for analysis in DPBS with 20% purified mouse IgG (Lampire Biological Laboratories) to minimize the adherence of target cells to hMDMs. Harvested cells were analyzed by flow cytometry with Cyto-Cal Count Control beads (Thermo Fisher) using an LSR II (BD Biosciences) flow cytometer to determine the absolute number of surviving viable CLL cells as previously described (8). In brief, after vigorously removing cells from well with pipette tip, cells were centrifuged to pellet and resuspended in 100 μL of 2% FBS-DPBS containing mouse antihuman antibodies to CD11b (clone ICRF44; BD Biosciences) and CD19 (clone HIB19; BioLegend) for 30 minutes. Cells were stained for viability with 1 nmol/L TO-PRO-3, washed with 2% FBS-DPBS, and resuspended in 2%FBS-DPBS. The absolute number of nonphagocytized B cells (B-cell count) was determined from the viable portion of the $CD11b^-PKH26^+$ cells in the CLL gate of the scatter plot (8). The increase in the mean number of CLL cells phagocytized due to mAb-induced ADCP was determined by subtracting the value achieved for no-mAb controls for each mAb experiment, to correct for nonspecific cell loss and mAb-independent phagocytosis.

The ability of each mAb to induce ADCP was evaluated by calculating the percentage of ADCP as previously described (8). In brief, the absolute number of nonphagocytized target B cells (B-cell count) was determined from the $CD11b^-PKH26^+$ cells in

Downloaded from http://aacrjournals.org/cancerimmunolres/article-pdf/6/10/1150/2343068/1150.pdf by guest on 23 April 2024

the CLL gate of the scatter plot. For comparison of mAb efficacy, the percentage of ADCP for each experiment was calculated as 100 × (1 − experimental B-cell count with mAb/control B-cell count without mAb). We have previously shown that there was no significant direct cytotoxic effects of any of the mAbs tested in the ADCP assays (8).

The role of complement activation in ADCP was determined by comparing ADCP in cultures using either C5-depleted serum or heat-inactivated C5-depleted serum. To ensure that heat inactivation prevented covalent binding of C3b to target cell membranes, we measured cell-bound C3-derived complement fragments using the FITC-labeled anti-C3b/iC3b 7C12 (ref. 40; kindly provided by Dr. Ronald P. Taylor) as previously described (41). For all of these experiments, CLL cells from 6 specimens were incubated with antibody and either active or heat-inactivated C5b-depleted serum for 1 hour in the presence of purified mouse IgG (2 mg/mL) to minimize nonspecific binding. C3b/iC3b binding was measured by flow cytometry and calculated as the geometric mean FITC fluorescence intensity of the viable CLL cell ($CD19^+CD5^+$) gate.

ADCC assay

Multiparametric flow cytometry–based ADCC assays, previously shown to reliably measure NK cell–mediated cytotoxicity and to be more sensitive than ^{51}chromium release assays (42), were used in this study. NK cell–enriched mononuclear cells were cryopreserved for a week between isolation and the assays to compare ADCC with ADCP to allow for maturation of hMDMs. NK cells were thawed, cultured overnight in RPMI-1640 supplemented with 10% FBS, penicillin, streptomycin, and L-glutamine (Gibco, Life Technologies) and checked for viability by trypan blue exclusion prior to use. The mean viability of these NK cells was 76% (range, 60%–81%), and the absolute viable NK cell count was used to establish a 5:1 NK:CLL cell ratio in the ADCC assays. Our preparatory experiments showed no significant differences in results of ADCC assays using fresh versus thawed NK cells. NK cells (2.5×10^5 in 100 μL) were equilibrated at 37°C with 95% humidity and 5% CO_2 for 1 hour. CLL cells (5×10^5 cells/mL) were simultaneously incubated in an upright 25-mL flask (CELLSTAR Greiner Bio-One) in AIM-V medium (Gibco, Life Technologies). Assays were initiated by adding 100 μL of the CLL cell suspension (5×10^4 cells) to the NK cell suspension to achieve an effector (NK cell) to target (CLL cell) ratio of 5:1. This ratio was selected because it achieved maximum ADCC in our preliminary studies. The test mAb (rituximab, ofatumumab, ocaratuzumab, or obinutuzumab) was immediately added in 50 μL of AIM-V to a final concentration of 10 μg/mL. The coculture was then incubated for 3 hours, after which the absolute number of remaining viable CLL cells was counted by flow cytometry using annexin V–FITC (BD Pharmingen), anti-CD19–PerCP (clone SJ25C1; BioLegend), anti-CD56–BUV395 (clone NCAM16.2; BD Biosciences), TO-PRO-3 (Life Technologies), and Cyto-Cal Count Control beads to examine 2.5×10^4 events. Cells in the CLL gate ($CD19^+CD56^-$) were considered viable if they were negative for expression of annexin V and did not stain with TO-PRO-3. The percentage of ADCC was calculated as 100 × (1 – experimental viable B-cell count/no-mAb control viable B-cell count). The cytotoxic capacity of NK cells (ADCC) and hMDMs (ADCP) was determined by dividing the absolute number of CLL cells undergoing mAb-induced apoptosis or phagocytosis by the number of effector cells.

Combination assays

Combination therapy assays were conducted to assess the effects on ADCP by hMDMs exposed to additional therapeutic agents used in the management of patients with CLL at clinically achievable and effective concentrations: ibrutinib (used at final concentration of 1 μmol/L), idelalisib (1 μmol/L), venetoclax (5 nmol/L; Selleckchem), bendamustine hydrochloride (10 μmol/L; Tocris Bioscience), dexamethasone (1 μmol/L), and 2-fluoroadenine 9-B-D-arabinofuranoside (F-ara-A, active metabolite of fludarabine; Sigma-Aldrich; 3 μmol/L), acalabrutinib (1 μmol/L), and ACP-319 (1 μmol/L) generously provided by Acerta Pharma, and umbralisib (TGR-1202; 1 μmol/L) generously provided by TG Therapeutics. hMDMs were preincubated with the drug of interest for 1 hour prior to initiation of the standard 3-hour ADCP assay at the same concentration as for the ADCP assay in the RPMI-1640 medium. All drugs were diluted with DMSO at 1,000-fold higher than the final assay test concentration. Upon completion of the 1-hour preincubation with the drugs, all ADCP assays were performed exactly as described above. Equivalent amounts of DMSO were added to controls. For these assays, each antibody–drug combination was compared with the no-antibody control with the same drug tested, and the percentage of ADCP was calculated as described for the ADCP assays.

Statistical methods

Linear mixed models were used to assess the relationship between ADCP and ADCC, while adjusting for mAb with a categorical fixed effect and accounting for correlations between data coming from the same subject with a subject-specific random intercept term. Spearman rank correlations were used to assess the relationship between ADCP and ADCC within each mAb individually. The effect of drug concentration on ADCP was modeled using mixed ANOVA with drug concentration and mAb treated as categorical fixed effects. The effect of various therapeutic agents on ADCP was similarly modeled via a categorical fixed effect. EC_{50} for each mAb was found by fitting nonlinear Hill equations, with the confidence intervals estimated by the empirical bootstrap method. Paired *t* tests were used to assess the change in ADCP under varying experimental conditions, including autologous versus allogeneic hMDMs and active versus heat-inactivated C5-depleted serum. Hypothesis tests were conducted at the 0.05 level of significance. Due to the exploratory nature of the analyses, we did not correct for multiple comparisons. Future studies will be done to verify promising results. SAS version 9.4 (SAS Institute, Inc.) was used for all analyses.

Results

ADCP is the high-capacity immune cellular cytotoxicity mechanism

To evaluate the relative efficacy of ADCC and ADCP, we conducted a series of parallel experiments, each of which used peripheral blood-derived NK and hMDM effector cells from one healthy blood donor sample and target CLL cells from one patient sample (Fig. 2). Each paired comparison used data derived from experiments done on the same day. For these 11 experiments, we used effector cells from 7 healthy human donors and CLL target cells from 9 patients. Healthy donor effector cells were used because CLL patient blood samples did not yield adequate numbers of NK cells for the planned ADCC assays. All experiments were done with a final mAb concentration of 10 μg/mL. ADCP of

Downloaded from http://aacrjournals.org/cancerimmunolres/article-pdf/6/10/1150/2343068/1150.pdf by guest on 23 April 2024

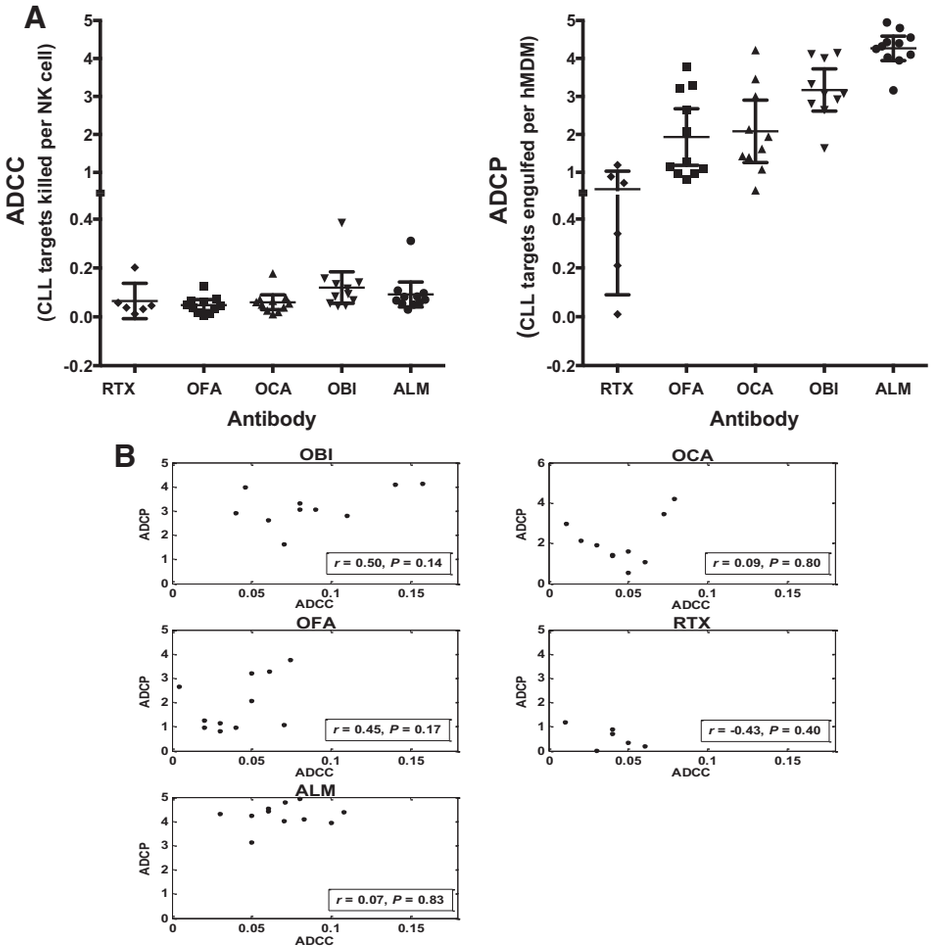

Figure 2.
Comparison of ADCC and ADCP. **A,** Healthy human blood-derived NK cells (5:1) and hMDMs (1:5) from 7 donor specimens were used to test mAb-induced ADCC and ADCP of CLL target cells from 9 patients in 11 independent paired experiments. The four CD20 mAbs rituximab (RTX), ofatumumab (OFA), ocaratuzumab (OCA), and obinutuzumab (OBI) and the CD52 mAb alemtuzumab (ALM) were all used at a final concentration of 10 μg/mL. The data shown are from 11 comparisons for OFA and ALM, 10 for OBI and OCA, and 6 for RTX. Means and 95% confidence intervals are shown. **B,** Dot plots of ADCC versus ADCP for each mAb were analyzed using Spearman rank correlations (r) with corresponding P value. $P < 0.05$ indicates statistical significance.

CLL target cells mediated by autologous hMDMs ($n = 16$) was compared with ADCP of the same CLL targets cells by hMDMs from healthy donors. No significant difference in ADCP was observed via a linear mixed model adjusted for antibody, and accounting for data coming from the same subject ($P = 0.35$). The average ADCP mediated by autologous versus healthy donor hMDMs by antibody was 46.1% versus 50.5% for obinutuzumab, 39.0% versus 42.4% for ocaratuzumab, 33.0% versus 38.9% for ofatumumab, and 31.6% versus 26% for rituximab, respectively.

NK cell ADCC (effector to target ratio of 5:1) killed ∼20% to 40% of the CD20 mAb-ligated CLL cell targets, translating to a cytotoxic capacity of ∼0.04 to 0.1 CLL cells killed per NK cell (Fig. 2A). By comparison, ADCP by hMDMs (effector to target ratio of 1:5) resulted in engulfment of ∼10% to 60% of CD20 mAb-ligated CLL cell targets, translating to a cytotoxic capacity of ∼0.5 to 3 phagocytized CLL cells per hMDM (Fig. 2A). Thus, CD20 mAb-mediated cytotoxicity of CLL cells per effector cell was >10-fold greater for ADCP compared with ADCC (paired one-sided t tests by antibody: rituximab $P = 0.019$, ofatumumab $P < 0.0001$, ocaratuzumab $P = 0.0002$, obinutuzumab $P < 0.0001$, alemtuzumab $P < 0.0001$). We emphasize that the effector/target ratios were 25-fold higher for the NK cell-mediated ADCC reaction, and it is, thus, evident that macrophage-mediated ADCP is the more effective killing process.

mAb induction of ADCC does not predict ADCP

We then analyzed our data to determine if the commonly accepted standard of mAb-induced ADCC (9, 20, 43) was a valid surrogate measurement for mAb-induced ADCP. To make these results more generalizable, we included the well established and clinically available prototypic humanized CD52 mAb alemtuzumab. Alemtuzumab (wild-type human IgG1κ) induced substantial ADCP (Fig. 2A; ref. 8) and is known to be effective at clearing CLL cells from the peripheral blood *in vivo* (44). Adjusting for antibody, no significant association between ADCP and ADCC was found ($P = 0.51$; Fig. 2A). Spearman rank correlations within the mAb for each of the 5 tested mAbs corroborated this lack of association (all $P > 0.14$; Fig. 2B). These data show that for any given tested mAb, the ability to induce ADCC does not predict ability to induce ADCP.

ADCP and mAb concentrations

To determine the mAb concentrations required to initiate and achieve maximum ADCP, we studied rituximab, ofatumumab, ocaratuzumab, and obinutuzumab at 0.01 to 10 μg/mL (Fig. 3). All mAb comparisons were performed in parallel on the same day using the same pair of autologous patient-derived hMDMs and target CLL cells derived from one patient sample. At the lowest tested mAb concentration, ocaratuzumab ($P < 0.0001$) and ofatumumab ($P = 0.0028$) induced significant ADCP compared

Downloaded from http://aacrjournals.org/cancerimmunolres/article-pdf/6/10/1150/2343068/1150.pdf by guest on 23 April 2024

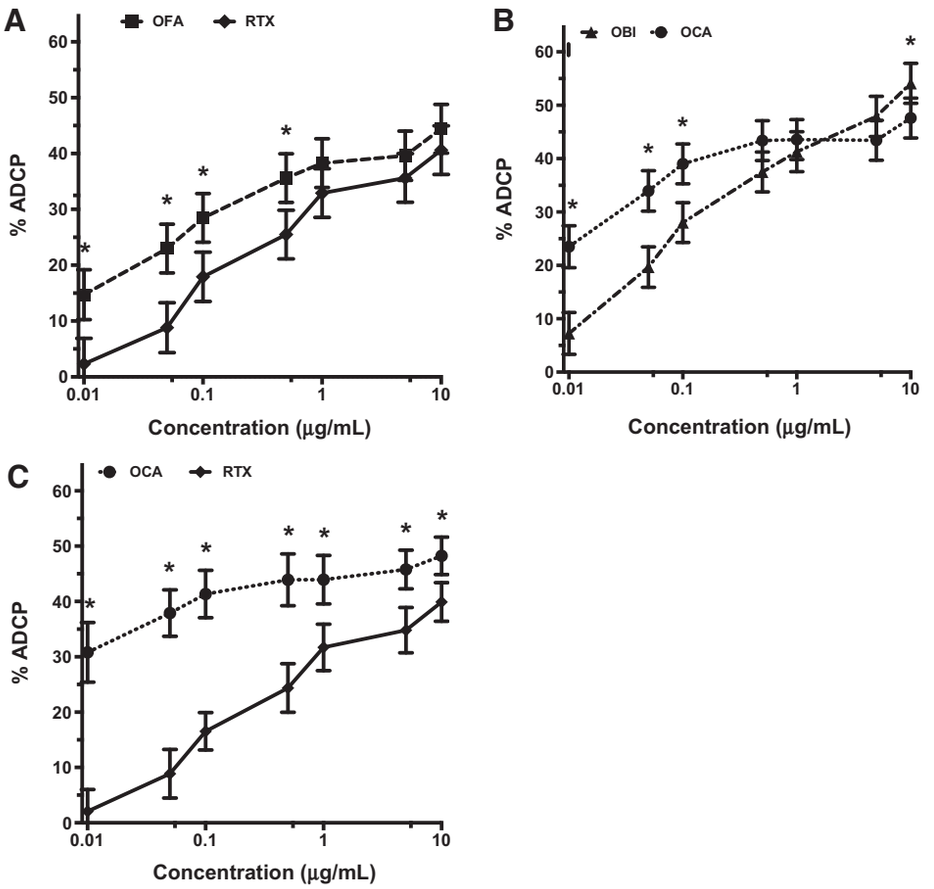

Figure 3.
CD20-binding efficiency and FcR affinity affect ADCP. ADCP was measured using mAb concentrations of 0.01 to 10 μg/mL and an hMDM:CLL of 1:5 in 31 independent experiments, each using a different CLL patient-derived blood sample. Data shown are mean ± SEM for each concentration, with a range of 11 to 19 data points for each concentration. ADCP was modeled using mixed ANOVA, with drug concentration and mAb as categorical fixed effects. Asterisks: significant differences ($P < 0.05$).
A, Comparison of mAbs with wild-type (WT) Fc [rituximab (RTX) vs. ofatumumab (OFA), $n = 14$].
B, Comparison of the Fc-modified mAbs [obinutuzumab (OBI) vs. ocaratuzumab (OCA), $n = 25$].
C, Comparison of higher CD20-binding efficiency and FcR-affinity OCA vs. lower CD20-binding efficiency and WT Fc RTX ($n = 17$).

with the no-mAb controls. In contrast, appreciably higher concentrations were required to induce ADCP with obinutuzumab (0.05 μg/mL, $P < 0.0001$) and rituximab (0.1 μg/mL, $P = 0.0004$). Ocaratuzumab had the lowest estimated EC_{50} [0.0080 μg/mL; 95% confidence interval (CI), 0.0035–0.0113], followed by ofatumumab (0.0459 μg/mL; 95% CI, 0.0216–0.0613), obinutuzumab (0.0493 μg/mL; 95% CI, 0.0326–0.0642), and rituximab (0.3151 μg/mL; 95% CI, 0.1952–0.4139). Confidence intervals demonstrated that the EC_{50} of ocaratuzumab was significantly lower than the EC_{50} for all the other mAbs tested and that the EC_{50} of rituximab was significantly higher than the EC_{50} of all the other mAbs ($P < 0.05$). No significant difference between the EC_{50} of obinutuzumab and ofatumumab was found.

We then compared the ADCP at lower mAb concentrations with that achieved at 10 μg/mL (Fig. 3). Ocaratuzumab- and rituximab-induced ADCP were significantly lower at 0.01 to 1 μg/mL, and obinutuzumab- and ofatumumab-induced ADCP were significantly lower at all concentrations <10 μg/mL. These data suggested that maximum ADCP was achieved for ocaratuzumab and rituximab at mAb concentrations between 1 and 5 μg/mL but was not achieved for obinutuzumab and ofatumumab at 5 μg/mL.

To further investigate the role of CD20 mAb ligand binding on ADCP, we compared high versus low CD20 binding efficiency of mAbs segregated by wild-type versus bioengineered Fc (Fig. 3). Comparing mAbs with wild-type Fc, the higher CD20-binding efficiency of ofatumumab induced significantly more ADCP than rituximab at mAb concentrations up to 0.5 μg/mL (Fig. 3A). These data strongly suggest an important role for CD20 binding efficacy in mediating CD20 mAb-induced ADCP. Comparison of the Fc-modified mAbs showed that the higher CD20-binding efficiency of ocaratuzumab induced significantly more ADCP than obinutuzumab at mAb concentrations up to 0.1 μg/mL, and obinutuzumab induced significantly more ADCP than ocaratuzumab at 10 μg/mL (Fig. 3B). These data support the role of CD20-binding efficiency for inducing ADCP.

CD20 mAb affinity for FcR is expected to influence synapse formation and, hence, ADCP. The CD20 mAbs studied have different CD20 binding affinities, limiting our ability to directly examine the role of FcR affinity. As an exploratory step, we directly compared ADCP induced by the Type I mAbs with the highest (ocaratuzumab) and lowest (rituximab) CD20 and FcR affinity. As shown in Fig. 3C, ocaratuzumab induced significantly higher ADCP than rituximab at all mAb concentrations tested. The differences between this comparison and that between ofatumumab and rituximab (Fig. 3A) suggest that increased FcR affinity could increase ADCP.

Complement activation can increase ADCP

Fragments of complement protein C3 (C3b/iC3/C3dg) covalently bind to mAb-opsonized target cell membranes and can ligate complement receptor 3 (CR3) on macrophages to form a complement synapse (Fig. 1). We compared ADCP in experiments using multiple pairs of single healthy donor sample-derived hMDMs and mAb-opsonized single patient CLL cells. The cells were then cultured with either active C5-deficient serum, which

Downloaded from http://aacrjournals.org/cancerimmunolres/article-pdf/6/10/1150/2343068/1150.pdf by guest on 23 April 2024

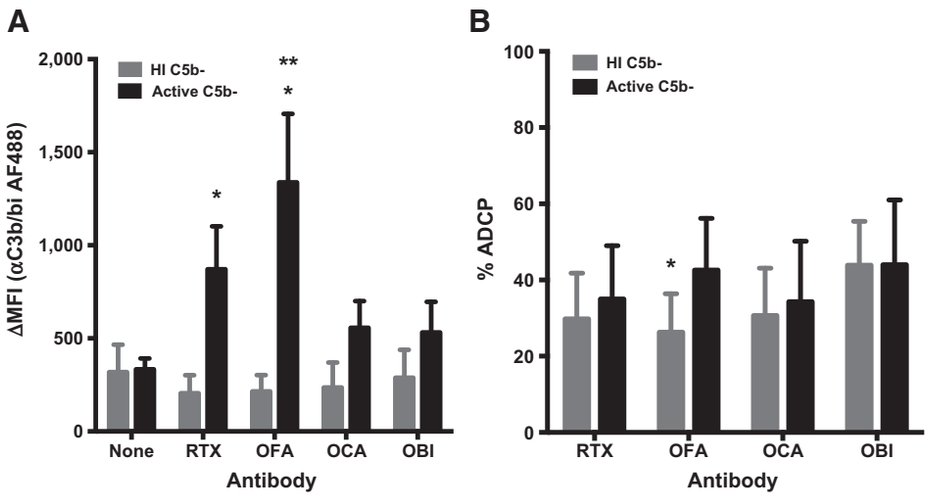

Figure 4.

Complement activation can increase ADCP. **A,** Covalent binding of C3b/iC3b to CLL cell membranes was measured in 6 CLL cell specimens in 2 independent experiments. C3b/iC3b binding induced by obinutuzumab (OBI), ocaratuzumab (OCA), ofatumumab (OFA), and rituximab (RTX) was measured in the presence of either C5-depleted human serum (active C5b-) or heat-inactivated C5-depleted human serum (HI C5b-) using the C3b/iC3b mAb 7C12 and represented as mean + SEM. Data were compared using paired *t* tests, with $P < 0.05$ indicating statistical significance (*, $P < 0.05$; **, $P = 0.0329$). **B,** ADCP of CLL ($n = 11$) cells by healthy donor hMDM ($n = 6$) was compared for each mAb (10 μg/mL) in assays using 10% active C5b- or HI C5b- serum (mean + SEM; $n = 13$, except OCA $n = 12$). Paired *t* tests were used to compare ADCP, with *, $P < 0.05$ indicating statistical significance.

generates C3, or heat-inactivated C5-deficient serum, which does not. As shown in Fig. 4A, rituximab, ofatumumab, obinutuzumab, and ocaratuzumab significantly increased C3b/iC3b binding to CLL cells in active compared with heat-inactivated C5-deficient serum as measured by ΔMFI ($P < 0.05$). Ofatumumab and rituximab were significantly more effective at generating CLL cell membrane-bound iC3b fragments than the Fc-engineered mAbs obinutuzumab and ocaratuzumab ($P < 0.05$). As expected (24, 26), ofatumumab generated significantly higher iC3b than rituximab ($P = 0.03$). Heat inactivation of C5-deficient serum significantly decreased ADCP induced by ofatumumab ($P = 0.0013$; Fig. 4B). These data demonstrate that effective complement activation by ofatumumab results in substantial iC3b fragment opsonization of target cells, likely leading to formation of complement synapses that enhance ADCP. The lower ADCP mediated by ofatumumab in heat-inactivated serum may be due to the fact that ofatumumab binds closer to the cell membrane, which tends to decrease phagocytosis compared with phagocytosis mediated by an mAb that binds further away from the cell membrane (45). Thus, opsonization with complement fragments (most effectively mediated by ofatumumab) leads to a significant increase in phagocytosis for this mAb.

Modulation of ADCP by targeted small-molecule inhibitors

We tested multiple drugs that have previously been combined with CD20 mAb treatment regimens for B-cell malignancies (29–31) to determine their effect on *in vitro* ADCP. These experiments used 16 pairs of autologous CLL patient-derived hMDMs and target cells from the same sample. To test hMDM toxicity, we added each drug to hMDM cultures for 4 hours and then measured hMDM counts and viability 24 hours later by flow cytometry using annexin V and TO-PRO-3. Paired *t* tests found no significant reduction in macrophage viability in the presence of any tested drug compared with DMSO control (all $P > 0.14$). The average macrophage viability in the presence of inhibitors was 80.7% for ibrutinib, 79.1% for acalabrutinib, 78.9% for idelalisib, 79.3% for ACP-319, and 77.5% for umbralisib compared with 79.5% macrophage viability for the no-inhibitor DMSO control.

Venetoclax (5 nmol/L), dexamethasone (1 μmol/L), bendamustine (10 μmol/L), and F-ara-A (3 μmol/L) did not significantly alter ADCP induced by rituximab, ofatumumab, obinutuzumab, or ocaratuzumab. In contrast, inhibitors targeting BTK and PI3Kδ (all used at a concentration of 1 μmol/L) decreased mAb-induced ADCP (Fig. 5). Ibrutinib ($P = 0.0116$) and ACP-319 ($P = 0.0035$) significantly decreased rituximab-induced ADCP (Fig. 5A). Rituximab-induced ADCP was suppressed significantly more by ibrutinib compared with acalabrutinib ($P = 0.0307$), and ibrutinib ($P = 0.0270$), idelalisib ($P = 0.0044$), and ACP-319 ($P = 0.0347$) significantly decreased ofatumumab-induced ADCP (Fig. 5B). Ibrutinib ($P = 0.0004$), idelalisib ($P < 0.0001$), ACP-319 ($P < 0.0001$), and umbralisib ($P = 0.0018$) significantly decreased ocaratuzumab-induced ADCP (Fig. 5C), and ocaratuzumab-induced ADCP was suppressed significantly more by idelalisib than umbralisib ($P = 0.0259$). All tested drugs significantly decreased obinutuzumab-induced ADCP (ibrutinib $P < 0.0001$, acalabrutinib $P = 0.0175$, idelalisib $P < 0.0001$, ACP-319 $P < 0.0001$, umbralisib $P = 0.0028$; Fig. 5D). Obinutuzumab-induced ADCP was suppressed significantly more by ibrutinib compared with acalabrutinib ($P < 0.0001$) and by idelalisib ($P = 0.0450$) and ACP-319 ($P = 0.0186$) compared with umbralisib.

In summary, ibrutinib and ACP-319 significantly decreased ADCP induced by all mAbs tested. Acalabrutinib significantly inhibited ADCP induced by obinutuzumab, but this effect was significantly less than that of ibrutinib. Idelalisib significantly inhibited ADCP induced by obinutuzumab, ocaratuzumab, and ofatumumab. Umbralisib significantly inhibited ADCP induced by obinutuzumab and ocaratuzumab, but this effect was significantly less than idelalisib. These results suggest that the BTK-specific inhibitor acalabrutinib and the novel PI3Kδ

Downloaded from http://aacrjournals.org/cancerimmunolres/article-pdf/6/10/1150/2343068/1150.pdf by guest on 23 April 2024

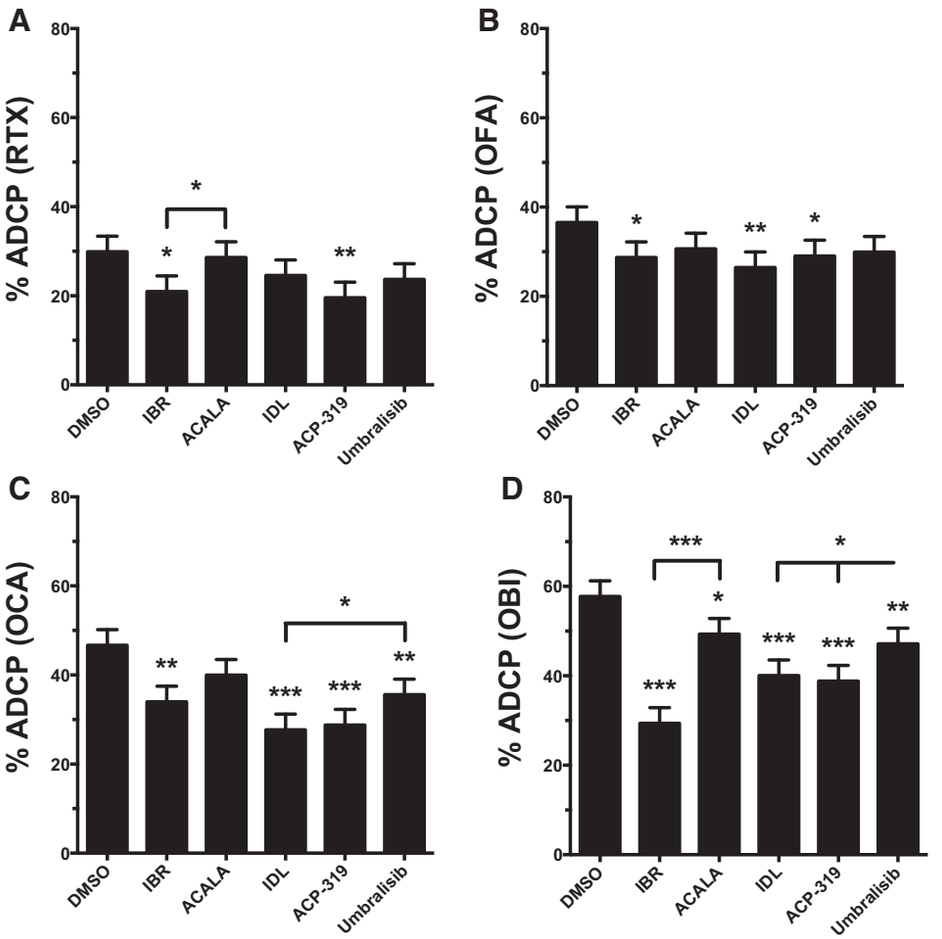

Figure 5.
Modulation of ADCP by drugs targeting the B-cell receptor signaling pathway. The effects of targeted small-molecule inhibitors of the B-cell receptor signaling pathway on ADCP were tested in 16 independent experiments using 16 pairs of CLL patient–derived hMDMs and CLL cells (mean + SEM). Autologous hMDMs were preincubated for 1 hour with either control (DMSO), ibrutinib (IBR), acalabrutinib (ACALA), idelalisib (IDL), ACP-319, or umbralisib (all at concentration of 1 μmol/L) before testing for mAb-induced (all used at a concentration of 10 μg/mL) ADCP. ADCP was modeled using mixed ANOVA, with inhibitors and mAbs as categorical fixed effects. $P < 0.05$ indicates statistical significance. **A,** Rituximab (RTX)-induced ADCP (IBR, *, $P = 0.0116$; IBR-ACALA, *, $P = 0.0307$; ACP-319, **, $P = 0.0035$). **B,** Ofatumumab (OFA)-induced ADCP (IBR, *, $P = 0.0270$; IDL, **, $P = 0.0044$; ACP-319, *, $P = 0.0347$). **C,** Ocaratuzumab (OCA)-induced ADCP (IBR, **, $P = 0.0004$; IDL, ***, $P < 0.0001$; IDL-umbralisib, *, $P = 0.0259$; ACP-319, ***, $P < 0.0001$; umbralisib, **, $P = 0.0018$). **D,** Obinutuzumab (OBI)-induced ADCP (IBR, ***, $P < 0.0001$; IBR-ACALA, ***, $P < 0.0001$; ACALA, *, $P = 0.0175$; IDL, ***, $P < 0.0001$; IDL-umbralisib, *, $P = 0.0450$; ACP-319, ***, $P < 0.0001$; ACP-319-umbralisib, *, $P = 0.0186$; umbralisib, **, $P = 0.0028$).

inhibitor umbralisib could be more suitable for combination therapy with CD20 mAbs in CLL.

Discussion

This study used primary hMDMs derived from either CLL patients or healthy donor blood in quantitative assays of ADCP, using primary CLL cells ligated by CD20 mAbs with distinct biological properties. We showed that ADCP was a high-capacity, innate immune cytotoxic mechanism that is more effective than NK cell ADCC in a primary human cell model. Our data showed that NK cell ADCC does not predict ADCP induced by CD20- or CD52-targeting mAbs and is, thus, not a surrogate measurement for mAb-induced cellular cytotoxicity. Preclinical analysis of the biochemical differences among available CD20 mAbs showed that the high CD20-binding efficiencies of mAbs ofatumumab and ocaratuzumab induced ADCP at drug concentrations that were lower than those achieved clinically. Fc engineering was associated with increased ADCP at higher mAb concentrations but also abrogated complement activation, an important mechanism for activating ADCP. The first-generation small-molecule inhibitors of BTK (ibrutinib) and PI3Kδ (idelalisib) were strong inhibitors of mAb ADCP. In contrast, the more specific BTK inhibitor acalabrutinib and novel PI3Kδ inhibitor umbralisib caused less inhibition of CD20 mAb-induced ADCP, and the BCL2 inhibitor venetoclax caused no significant inhibition. Our preclinical data provide a rationale for the design of novel approaches for the treatment of CLL and other B-cell malignancies using kinetically optimized mAb administration in combination with small-molecule targeted drugs selected to minimize inhibition of ADCP.

The primary *in vivo* mechanism of cellular cytotoxicity of circulating CD20 mAb-opsonized cells in mice is ADCP by fixed macrophages in the liver (13–15, 17). However, limited data on human *in vivo* CD20 mAb-mediated cellular cytotoxicity of circulating or tissue resident B cells are available. Human NK cells ($\sim 7 \times 10^{10}$) are largely restricted to the circulation with limited malignant tissue infiltration (46, 47). In contrast, $\sim 2 \times 10^{11}$ fixed macrophages are distributed widely throughout the body, including the sinusoids of the liver and spleen (46), meaning far more effector cell macrophages than NK effector cells are present, and the killing efficacy per cell favors macrophages. We and others have previously shown that hMDMs efficiently mediate ADCP of CD20 mAb-opsonized B cells (8, 16). This study showed that the average ADCC per NK cell is less than 10% of the ADCP mediated per hMDM. Based on these quantitative considerations, we, therefore, propose that ADCP is likely to be the major cytotoxic mechanism for CD20 mAbs in humans.

ADCC assays have been previously used as a surrogate measure of the cellular cytotoxicity of CD20 mAbs (20, 23, 43). Our data showed that NK cell ADCC did not predict ADCP capacity, a

Downloaded from http://aacrjournals.org/cancerimmunolres/article-pdf/6/10/1150/2343068/1150.pdf by guest on 23 April 2024

conclusion compatible with published data stating that the distance of mAb binding epitopes from the cell membrane differentially affects the ability to activate ADCC (more proximal) or ADCP (more distal; ref. 45). Given the predominant role of ADCP in mediating mAb cytotoxicity and the lack of proportionality between ADCC and ADCP, we propose that quantitative ADCP assays should be used to evaluate mAb-mediated cellular cytotoxicity.

Having confirmed the critical role of ADCP in mediating mAb cytotoxicity, we proceeded to investigate the effects of the properties that were selected or engineered into next-generation CD20 mAbs to improve ADCC. Limited published quantitative data exist on the consequences of modulation of CD20 and FcR affinity for CD20 mAb ADCP. We showed that the high CD20 binding efficiency of next-generation mAbs ofatumumab and ocaratuzumab induced ADCP at a concentration of <0.01 μg/mL. The lower CD20 binding efficiency mAbs had threshold ADCP induction concentrations that were >5-fold higher for obinutuzumab (0.05 μg/mL) and >10-fold higher for rituximab (0.1 μg/mL). Conventional doses of either intravenously or subcutaneously administered rituximab are designed to achieve serum trough concentrations >10 μg/mL (48), which exceeds the threshold *in vitro* concentration by ∼100-fold. These data suggest that conventionally used mAb doses are larger than required for ADCP in patients with circulating malignant B cells. However, additional studies will be required to determine the threshold concentrations for ADCP in malignant lymphoid tissue.

The cytotoxicity of conventional chemotherapy drugs increases with higher drug concentrations until all sensitive target cells are killed. In contrast, the cytotoxicity of mAb-induced ADCP can be limited by macrophage phagocytic capacity (8). This study showed that for mAb concentration increments above the threshold for induction of ADCP, progressively smaller increases in cytotoxicity were seen for each dose increase, with no significant increase in ADCP for ocaratuzumab and rituximab between 5 and 10 μg/mL. These data suggest that CD20 mAb-induced ADCP is a finite-capacity cytotoxic mechanism and that increasing mAb concentrations above the level required to achieve maximum efficacy will not improve clinical outcome for patients.

Covalent binding of complement C3 activation fragments to target cell membranes provides an additional target cell binding site for phagocytic macrophages via CR3. Limited data on the role of the complement iC3b–CR3 phagocytic synapse in next-generation αCD20 mAb-mediated ADCP are available. Ofatumumab, a potent activator of complement, generated the highest level of CLL cell-bound C3 activation fragments, and heat inactivation of serum significantly decreased ofatumumab-mediated ADCP. In contrast, rituximab complement activation was not sufficient to significantly increase ADCP. These findings suggest that high complement activation can be an important mediator of mAb-induced ADCP. In contrast, the Fc engineering used to generate ocaratuzumab and obinutuzumab prevents these mAbs from generating complement phagocytic synapses.

CLL and other indolent B-cell malignancies remain incurable with conventional therapies. Improvements in treatment outcomes will require rational combinations of targeted therapies. Studies of drug combinations suggest that small-molecule inhibitors of BTK and PI3Kδ, used in regimens designed to continuously block target enzymatic activity, could decrease cellular cytotoxicity mediated by CD20 mAbs (32–34). We now report a comprehensive study of the effects on hMDM ADCP of drugs that have been combined with CD20 mAbs in the treatment of CLL. Preincubation of hMDMs with therapeutic concentrations of dexamethasone, alkylating agents, purine analogues, and the BCL2 inhibitor venetoclax did not significantly alter CD20 mAb-mediated ADCP. In contrast, we confirmed in a quantitative assay that the first-generation inhibitors of BTK (ibrutinib) and PI3Kδ (idelalisib) significantly inhibited ADCP. The BTK-specific inhibitor acalabrutinib did not significantly decrease ADCP-mediated by ocaratuzumab, ofatumumab, or rituximab and caused significantly less inhibition of obinutuzumab-induced ADCP than ibrutinib. This finding suggests that ibrutinib's off-target activities (e.g., inhibition of non-BTK TEC family molecules or other kinases) could have an important role in mediating ADCP, as previously reported using nonquantitative ADCP assays (35). The next-generation PI3Kδ inhibitor umbralisib did not significantly inhibit ADCP induced by ofatumumab or rituximab and caused significantly less inhibition of ADCP induced by obinutuzumab and ocaratuzumab than idelalisib. The reason for this difference is not known, and limited data exist on the relative PI3Kδ selectivity of umbralisib and idelalisib, with at least one published study showing no significant difference (49). The same study shows that umbralisib has additional activities, including inhibition of Casein Kinase-1ε (49) that could modulate the effect of this drug on hMDM-mediated ADCP. These data are important for both understanding the molecular pathways controlling ADCP and for designing future trials of combination therapy to improve therapeutic outcomes.

This study used assays that do not necessarily inform on *in vivo* human activity. The translational value of our data could also be limited by the sparse knowledge of the tissue levels of CD20 mAb achieved in patients with B-cell malignancies and the ADCP capacity of tumor-associated macrophages in lymphomatous tissue. Our studies on drugs tested in combination therapy used only limited durations of exposure to hMDMs, and these drugs could be more toxic to tissue macrophages *in vivo*. However, the drugs tested all have relatively short half-lives *in vivo*, so the model used was reasonable. We also only tested FDA-approved and later-stage development drugs that could be available for use in clinical trials and did not endeavor to examine new drugs to optimize ADCP in this study or test a range of concentrations of modifying drugs. These analyses are planned as future research goals.

In conclusion, our study showed that quantitative ADCP should be the standard assay for evaluation of the cellular cytotoxicity of CD20 mAbs. Modification of variable and Fc regions in next-generation CD20 mAbs can increase FcR-mediated ADCP, while decreasing complement-mediated ADCP. ADCP is activated by CD20 mAbs at considerably lower concentrations than achieved by standard doses, suggesting that mAb regimen modifications, including a higher frequency/lower dose approach, should be further explored to increase efficacy and convenience and decrease toxicity and cost (50–53). Targeted small-molecule inhibitors used to treat B-cell malignancies have different mAb-specific effects on CD20-induced ADCP. Less ADCP inhibition was seen using more specific BTK and novel PI3Kδ inhibitors, and no significant inhibition was seen with the BCL2 inhibitor venetoclax. These data could be useful in understanding the control and capacity of physiologic, pathologic, and therapeutic ADCP and for designing more effective and less toxic treatments for B-cell malignancies. Our preclinical data have been used to design a trial for initial treatment of progressive CLL using standard dose acalabrutinib and high-frequency/low-dose subcutaneous

Downloaded from http://aacrjournals.org/cancerimmunolres/article-pdf/6/10/1150/2343068/1150.pdf by guest on 23 April 2024

rituximab (50 mg twice a week for 6 months) that could be opened by the end of 2018.

Disclosure of Potential Conflicts of Interest

C.C. Chu has ownership interest (including stock, patents, etc.) in Pfizer, Inc. No potential conflicts of interest were disclosed by the other authors.

Authors' Contributions

Conception and design: K.R. VanDerMeid, C.S. Zent
Development of methodology: K.R. VanDerMeid, M.R. Elliott, C.S. Zent
Acquisition of data (provided animals, acquired and managed patients, provided facilities, etc.): K.R. VanDerMeid, C.S. Zent
Analysis and interpretation of data (e.g., statistical analysis, biostatistics, computational analysis): K.R. VanDerMeid, M.R. Elliott, A.M. Baran, C.C. Chu, C.S. Zent
Writing, review, and/or revision of the manuscript: K.R. VanDerMeid, M.R. Elliott, A.M. Baran, P.M. Barr, C.C. Chu, C.S. Zent
Administrative, technical, or material support (i.e., reporting or organizing data, constructing databases): K.R. VanDerMeid, C.C. Chu, C.S. Zent
Study supervision: C.S. Zent

Acknowledgments

The authors thank Drs. Ronald P. Taylor and Margaret Lindorfer for providing guidance, review, and reagents and Sharon Lewinski RN and Tania Orzol NP for assisting with specimen collection and CLL patients at Wilmot Cancer Institute for their participation in our research efforts and donation of specimens. We thank Mentrik Biotech for providing ocaratuzumab, TG Therapeutics for providing umbralisib (TGR-1202), Acerta Pharma for providing acalabrutinib and ACP-319, and the New York-Penn region of the American Red Cross for supplying healthy donor leukocytes.

This study was funded in part by the University of Rochester's Wilmot Foundation, a University of Rochester Research Award, grant funding from Acerta Pharma and Mentrik Biotech, and a generous gift from Ms. Elizabeth Aaron.

The costs of publication of this article were defrayed in part by the payment of page charges. This article must therefore be hereby marked *advertisement* in accordance with 18 U.S.C. Section 1734 solely to indicate this fact.

Received May 15, 2018; revised June 19, 2018; accepted August 3, 2018; published first August 8, 2018.

References

1. Coiffier B, Lepage E, Briere J, Herbrecht R, Tilly H, Bouabdallah R, et al. CHOP chemotherapy plus rituximab compared with CHOP alone in elderly patients with diffuse large-B-cell lymphoma. N Engl J Med 2002; 346:235–42.
2. Burmester GR, Feist E, Dorner T. Emerging cell and cytokine targets in rheumatoid arthritis. Nat Rev Rheumatol 2014;10:77–88.
3. Clynes R, Towers T, Presta L, Ravetch J. Inhibitory Fc receptors modulate in vivo cytoxicity against tumor targets. Nat Med 2000;6:443–6.
4. Kennedy AD, Solga MD, Schuman TA, Chi AW, Lindorfer MA, Sutherland WM, et al. An anti-C3b(i) mAb enhances complement activation, C3b(i) deposition, and killing of CD20+ cells by rituximab. Blood 2003;101: 1071–9.
5. Zent CS, Secreto CR, Laplant BR, Bone ND, Call TG, Shanafelt TD, et al. Direct and complement dependent cytotoxicity in CLL cells from patients with high-risk early-intermediate stage chronic lymphocytic leukemia (CLL) treated with alemtuzumab and rituximab. Leuk Res 2008;32: 1849–56.
6. Alduaij W, Ivanov A, Honeychurch J, Cheadle EJ, Potluri S, Lim SH, et al. Novel type II anti-CD20 monoclonal antibody (GA101) evokes homotypic adhesion and actin-dependent, lysosome-mediated cell death in B-cell malignancies. Blood 2011;117:4519–29.
7. Bologna L, Gotti E, Manganini M, Rambaldi A, Intermesoli T, Introna M, et al. Mechanism of action of type II, glycoengineered, anti-CD20 monoclonal antibody GA101 in B-chronic lymphocytic leukemia whole blood assays in comparison with rituximab and alemtuzumab. J Immunol 2011;186:3762–9.
8. Church AK, VanDerMeid KR, Baig NA, Baran AM, Witzig TE, Nowakowski GS, et al. Anti-CD20 monoclonal antibody-dependent phagocytosis of chronic lymphocytic leukaemia cells by autologous macrophages. Clin Exp Immunol 2016;183:90–101.
9. Reff ME, Carner K, Chambers KS, Chinn PC, Leonard JE, Raab R, et al. Depletion of B cells in vivo by a chimeric mouse human monoclonal antibody to CD20. Blood 1994;83:435–45.
10. Beum PV, Lindorfer MA, Taylor RP. Within peripheral blood mononuclear cells, antibody-dependent cellular cytotoxicity of rituximab-opsonized Daudi cells is promoted by NK cells and inhibited by monocytes due to shaving. J Immunol 2008;181:2916–24.
11. Valgardsdottir R, Cattaneo I, Klein C, Introna M, Figliuzzi M, Golay J. Human neutrophils mediate trogocytosis rather than phagocytosis of CLL B cells opsonized with anti-CD20 antibodies. Blood 2017;129:2636–44.
12. Uchida J, Hamaguchi Y, Oliver JA, Ravetch JV, Poe JC, Haas KM, et al. The innate mononuclear phagocyte network depletes B lymphocytes through Fc receptor-dependent mechanisms during anti-CD20 antibody immunotherapy. J Exp Med 2004;199:1659–69.
13. Minard-Colin V, Xiu Y, Poe JC, Horikawa M, Magro CM, Hamaguchi Y, et al. Lymphoma depletion during CD20 immunotherapy in mice is mediated by macrophage FcgammaRI, FcgammaRIII, and FcgammaRIV. Blood 2008;112:1205–13.
14. Montalvao F, Garcia Z, Celli S, Breart B, Deguine J, Van Rooijen N, et al. The mechanism of anti-CD20-mediated B cell depletion revealed by intravital imaging. J Clin Invest 2013;123:5098–103.
15. Gul N, Babes L, Siegmund K, Korthouwer R, Bogels M, Braster R, et al. Macrophages eliminate circulating tumor cells after monoclonal antibody therapy. J Clin Invest 2014;124:812–23.
16. Weiskopf K, Weissman IL. Macrophages are critical effectors of antibody therapies for cancer. mAbs 2015;7:303–10.
17. Grandjean CL, Montalvao F, Celli S, Michonneau D, Breart B, Garcia Z, et al. Intravital imaging reveals improved Kupffer cell-mediated phagocytosis as a mode of action of glycoengineered anti-CD20 antibodies. Sci Rep 2016;6:34382.
18. Schreiber AD, Frank MM. Role of antibody and complement in the immune clearance and destruction of erythrocytes. I. In vivo effects of IgG and IgM complement-fixing sites. J Clin Invest 1972;51:575–82.
19. de Back DZ, Kostova EB, van Kraaij M, van den Berg TK, van Bruggen R. Of macrophages and red blood cells; a complex love story. Front Physiol 2014;5:9.
20. Mossner E, Brunker P, Moser S, Puntener U, Schmidt C, Herter S, et al. Increasing the efficacy of CD20 antibody therapy through the engineering of a new type II anti-CD20 antibody with enhanced direct and immune effector cell-mediated B-cell cytotoxicity. Blood 2010;115: 4393–402.
21. Tobinai K, Ogura M, Kobayashi Y, Uchida T, Watanabe T, Oyama T, et al. Phase I study of LY2469298, an Fc-engineered humanized anti-CD20 antibody, in patients with relapsed or refractory follicular lymphoma. Cancer Sci 2011;102:432–8.
22. Forero-Torres A, de Vos S, Pohlman BL, Pashkevich M, Cronier DM, Dang NH, et al. Results of a phase 1 study of AME-133v (LY2469298), an Fc-engineered humanized monoclonal anti-CD20 antibody, in FcgammaRIIIa-genotyped patients with previously treated follicular lymphoma. Clin Cancer Res 2012;18:1395–403.
23. Maloney DG, Grillo-Lopez AJ, White CA, Bodkin D, Schilder RJ, Neidhart JA, et al. IDEC-C2B8 (Rituximab) anti-CD20 monoclonal antibody therapy in patients with relapsed low-grade non-Hodgkin's lymphoma. Blood 1997;90:2188–95.
24. Teeling JL, French RR, Cragg MS, van den Brakel J, Pluyter M, Huang H, et al. Characterization of new human CD20 monoclonal antibodies with potent cytolytic activity against non-Hodgkin lymphomas. Blood 2004;104: 1793–800.
25. Lindorfer MA, Bakker JM, Parren PW, Taylor RP. Ofatumumab (Arzerra): a next-generation human therapeutic CD20 antibody with potent complement-dependent cytotoxicity. In: Dubel S, Reichert J M, editor. Handbook of Therapeutic Antibodies: Wiley; 2014. p 1733.

Downloaded from http://aacrjournals.org/cancerimmunolres/article-pdf/6/10/1150/2343068/1150.pdf by guest on 23 April 2024

26. Baig NA, Taylor RP, Lindorfer MA, Church AK, Laplant BR, Pavey ES, et al. Complement dependent cytotoxicity (CDC) in chronic lymphocytic leukemia (CLL): Ofatumumab enhances alemtuzumab CDC and reveals cells resistant to activated complement. Leuk Lymphoma 2012;53: 2218–27.
27. Lukacsi S, Nagy-Balo Z, Erdei A, Sandor N, Bajtay Z. The role of CR3 (CD11b/CD18) and CR4 (CD11c/CD18) in complement-mediated phagocytosis and podosome formation by human phagocytes. Immunol Lett 2017;189:64–72.
28. Lee CH, Romain G, Yan W, Watanabe M, Charab W, Todorova B, et al. IgG Fc domains that bind C1q but not effector Fcgamma receptors delineate the importance of complement-mediated effector functions. Nat Immunol 2017;18:889–98.
29. Furman RR, Sharman JP, Coutre SE, Cheson BD, Pagel JM, Hillmen P, et al. Idelalisib and rituximab in relapsed chronic lymphocytic leukemia. N Engl J Med 2014;370:997–1007.
30. Burger JA, Keating MJ, Wierda WG, Hartmann E, Hoellenriegel J, Rosin NY, et al. Safety and activity of ibrutinib plus rituximab for patients with high-risk chronic lymphocytic leukaemia: a single-arm, phase 2 study. Lancet Oncol 2014;15:1090–9.
31. Seymour JF, Ma S, Brander DM, Choi MY, Barrientos J, Davids MS, et al. Venetoclax plus rituximab in relapsed or refractory chronic lymphocytic leukaemia: a phase 1b study. Lancet Oncol 2017;18:230–40.
32. Kohrt HE, Sagiv-Barfi I, Rafiq S, Herman SE, Butchar JP, Cheney C, et al. Ibrutinib antagonizes rituximab-dependent NK cell-mediated cytotoxicity. Blood 2014;123:1957–60.
33. Da Roit F, Engelberts PJ, Taylor RP, Breij EC, Gritti G, Rambaldi A, et al. Ibrutinib interferes with the cell-mediated anti-tumor activities of therapeutic CD20 antibodies: implications for combination therapy. Haematologica 2015;100:77–86.
34. Borge M, Almejun MB, Podaza E, Colado A, Fernandez Grecco H, Cabrejo M, et al. Ibrutinib impairs the phagocytosis of rituximab-coated leukemic cells from chronic lymphocytic leukemia patients by human macrophages. Haematologica 2015;100:e140–2.
35. Golay J, Ubiali G, Introna M. The specific BTK inhibitor acalabrutinib (ACP-196) shows favorable in vitro activity against chronic lymphocytic leukemia B-cells with CD20 antibodies. Haematologica 2017;102: e400–3.
36. Barf T, Covey T, Izumi R, van de Kar B, Gulrajani M, van Lith B, et al. Acalabrutinib (ACP-196): a covalent bruton tyrosine kinase inhibitor with a differentiated selectivity and in vivo potency profile. J Pharmacol Exp Ther 2017;363:240–52.
37. Hallek M, Cheson BD, Catovsky D, Caligaris-Cappio F, Dighiero G, Dohner H, et al. Guidelines for the diagnosis and treatment of chronic lymphocytic leukemia: a report from the International Workshop on Chronic Lymphocytic Leukemia (IWCLL) updating the National Cancer Institute-Working Group (NCI-WG) 1996 guidelines. Blood 2008;111: 5446–56.
38. Neron S, Dussault N, Racine C. Whole-blood leukoreduction filters are a source for cryopreserved cells for phenotypic and functional investigations on peripheral blood lymphocytes. Transfusion 2006;46:537–44.
39. Peytour Y, Villacreces A, Chevaleyre J, Ivanovic Z, Praloran V. Discarded leukoreduction filters: a new source of stem cells for research, cell engineering and therapy? Stem Cell Res 2013;11:736–42.
40. Lindorfer MA, Jinivizian HB, Foley PL, Kennedy AD, Solga MD, Taylor RP. B cell complement receptor 2 transfer reaction. J Immunol 2003;170: 3671–8.
41. Baig NA, Taylor RP, Lindorfer MA, Church AK, LaPlant BR, Pettinger AM, et al. Induced resistance to ofatumumab-mediated cell clearance mechanisms, including complement-dependent cytotoxicity, in chronic lymphocytic leukemia. J Immunol 2014;192:1620–9.
42. Kim GG, Donnenberg VS, Donnenberg AD, Gooding W, Whiteside TL. A novel multiparametric flow cytometry-based cytotoxicity assay simultaneously immunophenotypes effector cells: comparisons to a 4 h 51Cr-release assay. J Immunol Methods 2007;325:51–66.
43. Cheney CM, Stephens DM, Mo X, Rafiq S, Butchar J, Flynn JM, et al. Ocaratuzumab, an Fc-engineered antibody demonstrates enhanced antibody-dependent cell-mediated cytotoxicity in chronic lymphocytic leukemia. mAbs 2014;6:749–55.
44. Osterborg A, Fassas AS, Anagnostopoulos A, Dyer MJ, Catovsky D, Mellstedt H. Humanized CD52 monoclonal antibody Campath-1H as first-line treatment in chronic lymphocytic leukaemia. Br J Haematol 1996;93:151–3.
45. Cleary KLS, Chan HTC, James S, Glennie MJ, Cragg MS. Antibody distance from the cell membrane regulates antibody effector mechanisms. J Immunol 2017;198:3999–4011.
46. Freitas RA. Basic capabilities. Nanomedicine, Volume I. Georgetown, TX: Landes Bioscience; 1999.
47. Ames E, Murphy WJ. Advantages and clinical applications of natural killer cells in cancer immunotherapy. Cancer Immunol Immunother 2014;63: 21–8.
48. Salar A, Avivi I, Bittner B, Bouabdallah R, Brewster M, Catalani O, et al. Comparison of subcutaneous versus intravenous administration of rituximab as maintenance treatment for follicular lymphoma: results from a two-stage, phase IB study. J Clin Oncol 2014;32:1782–91.
49. Deng C, Lipstein MR, Scotto L, Jirau Serrano XO, Mangone MA, Li S, et al. Silencing c-Myc translation as a therapeutic strategy through targeting PI3Kdelta and CK1epsilon in hematological malignancies. Blood 2017; 129:88–99.
50. Williams ME, Densmore JJ, Pawluczkowycz AW, Beum PV, Kennedy AD, Lindorfer MA, et al. Thrice-weekly low-dose rituximab decreases CD20 loss via shaving and promotes enhanced targeting in chronic lymphocytic leukemia. J Immunol 2006;177:7435–43.
51. Aue G, Lindorfer MA, Beum PV, Pawluczkowycz AW, Vire B, Hughes T, et al. Fractionated subcutaneous rituximab is well-tolerated and preserves CD20 expression on tumor cells in patients with chronic lymphocytic leukemia. Haematologica 2010;95:329–32.
52. Zent CS, Taylor RP, Lindorfer MA, Beum PV, Laplant B, Wu W, et al. Chemoimmunotherapy for relapsed/refractory and progressive 17p13 deleted chronic lymphocytic leukemia (CLL) combining pentostatin, alemtuzumab, and low dose rituximab is effective and tolerable and limits loss of CD20 expression by circulating CLL cells. Am J Hematol 2014; 89:757–65.
53. Zent CS, Wang XV, Ketterling RP, Hanson CA, Libby EN, Barrientos JC, et al. A phase II randomized trial comparing standard and low dose rituximab combined with alemtuzumab as initial treatment of progressive chronic lymphocytic leukemia in older patients: a trial of the ECOG-ACRIN Cancer Research Group (E1908). Am J Hematol 2016;91:308–12.

Downloaded from http://aacrjournals.org/cancerimmunolres/article-pdf/6/10/1150/2343068/1150.pdf by guest on 23 April 2024